One-Year Longitudinal Assessment of Patients With CMT1A Using Quantitative MRI

Etienne Fortanier, Marc Adrien Hostin, Constance Michel, Emilien Delmont, Marc-Emmanuel Bellemare, Maxime Guye, David Bendahan, Shahram Attarian

One-year longitudinal assessment of CMT1A patients using Quantitative MRI

Manuscript Number: WNL-2023-005797R2

Authors:
Etienne Fortanier[1]; Marc Adrien Hostin[2]; Constance Michel[3]; Emilien Delmont[1]; Marc-Emmanuelle Bellemare[4]; Maxime Guye[2]; David Bendahan[2]; Shahram Attarian[1]

1. Reference Center for Neuromuscular Diseases and ALS, La Timone University Hospital, Aix-Marseille University, Marseille, France; 2. Center for Magnetic Resonance in Biology and Medicine, Aix-Marseille University, UMR CNRS 7339, Marseille, France; 3. Aix Marseille Univ, CNRS, CRMBM, UMR 7339, Marseille, France; 4. Aix Marseille University, CNRS, LIS, Marseille, France

Corresponding Author: Etienne Fortanier

Group Authorship: No. There is no study group involved in our research
Group Name:

Contributions:
Etienne Fortanier: Drafting/revision of the manuscript for content, including medical writing for content; Major role in the acquisition of data; Study concept or design; Analysis or interpretation of data; Marc Adrien Hostin: Major role in the acquisition of data; Analysis or interpretation of data; Constance Michel: Major role in the acquisition of data; Emilien Delmont: Major role in the acquisition of data; Study concept or design; Marc-Emmanuelle Bellemare: Study concept or design; Maxime Guye: Study concept or design; David Bendahan: Drafting/revision of the manuscript for content, including medical writing for content; Major role in the acquisition of data; Study concept or design; Analysis or interpretation of data; Shahram Attarian: Drafting/revision of the manuscript for content, including medical writing for content; Major role in the acquisition of data; Study concept or design; Analysis or interpretation of data;

Abstract: Background and Objectives: Intramuscular fat fraction (FF) assessed using quantitative MRI (qMRI) has emerged as one of the few responsive outcome measures in CMT1A suitable for future clinical trials. This study aimed to identify the relevance of multiple qMRI biomarkers for tracking longitudinal changes in CMT1A and to assess correlations between MRI metrics and clinical parameters. Methods: qMRI was performed in CMT1A patients at two time points, a year apart and various metrics were extracted from three-dimensional volumes of interest at thigh and leg levels. A semi-automated segmentation technique was used, enabling the analysis of central slices as well as a larger 3D muscle volume. Metrics included: proton density (PD), magnetization transfer ratio (MTR) and intramuscular fat fraction (FF). The sciatic and tibial nerves were also assessed. Disease severity was gauged using CMTNSv2, CMTES, ONLS scores, and MRC muscle strength. Results: Twenty-four patients were included. FF significantly rose in the 3D volume at both thigh (+1.04 {plus minus} 2.19%, p=0.041) and leg (+1.36 {plus minus} 1.87%, p=0.045) levels. The 3D analyses unveiled a length-dependent gradient in FF, ranging from 22.61 {plus minus}10.17% to 26.17 {plus minus} 10.79% at leg level. There was noticeable variance in longitudinal changes between muscles: +3.17 {plus minus} 6.86% (p=0.028) in the tibialis anterior compared to 0.37 {plus minus}4.97% (p=0.893) in the gastrocnemius medialis. MTR across the entire thigh volume showed a significant decline between the two time-points: -2.75 {plus minus} 6.58 (p=0.049), while no significant differences were noted for the 3D muscle volume and PD. No longitudinal changes were observed in any nerve metric. Potent correlations were identified between FF and primary clinical measures: CMTNSv2 (rho=0.656; p=0.001) and MRC in the lower limbs (rho=-0.877; p<0.001). Discussion: Our results further support that qMRI is a promising tool for following up longitudinal changes in CMT1A patients, FF being the paramount MRI metric for both thigh and leg regions. It's crucial to scrutinize the post-imaging data extraction methods considering that annual changes are minimal (around +1.5%). Given the varied FF distribution, the existence of a length-dependent gradient, and the differential fatty involution across muscles, 3D volume analysis appeared more suitable than single slice analysis.

One-year longitudinal assessment of CMT1A patients using Quantitative MRI

AUTHORS

Etienne Fortanier (MD)[a], Marc Adrien Hostin (Msc)[b], Constance Michel[b] (PhD), Emilien Delmont (MD, PhD)[a,c], Marc-Emmanuel Bellemare (PhD)[d], Maxime Guye (MD, PhD)[b], David Bendahan (PhD)[b], Shahram Attarian (MD, PhD)[a,e].

AFFILIATIONS:

[a] *Reference Center for Neuromuscular Diseases and ALS, La Timone University Hospital, Aix-Marseille University, Marseille, France*
[b] *Center for Magnetic Resonance in Biology and Medicine, Aix-Marseille University, UMR CNRS 7339, Marseille, France*
[c] *Aix-Marseille University, UMR 7286, Medicine Faculty, Marseille, France*
[d] *Aix Marseille University, CNRS, LIS, Marseille, France*
[e] *Aix-Marseille University, Inserm, GMGF, Marseille, France*

CORRESPONDING AUTHOR:

Etienne FORTANIER

Reference Center for Neuromuscular Diseases and ALS, La Timone University Hospital, Aix-Marseille University, 264 rue Saint Pierre, 13385 Marseille, France
Etienne.fortanier@ap-hm.fr
Tel: +33 4 91 38 65 79; Fax: + 33 4 91 42 68 55

TOTAL WORD COUNT: 3358

KEYWORDS: MRI, CMT1A, QUANTITATIVE, BIOMARKERS, FAT FRACTION, LONGITUDINAL, IMAGING

ABSTRACT

Background and Objectives: Intramuscular fat fraction (FF) assessed using quantitative MRI (qMRI) has emerged as one of the few responsive outcome measures in CMT1A suitable for future clinical trials. This study aimed to identify the relevance of multiple qMRI biomarkers for tracking longitudinal changes in CMT1A and to assess correlations between MRI metrics and clinical parameters.

Methods: qMRI was performed in CMT1A patients at two time points, a year apart and various metrics were extracted from three-dimensional volumes of interest at thigh and leg levels. A semi-automated segmentation technique was used, enabling the analysis of central slices as well as a larger 3D muscle volume. Metrics included: proton density (PD), magnetization transfer ratio (MTR) and intramuscular fat fraction (FF). The sciatic and tibial nerves were also assessed. Disease severity was gauged using CMTNSv2, CMTES, ONLS scores, and MRC muscle strength.

Results: Twenty-four patients were included. FF significantly rose in the 3D volume at both thigh (+1.04 ± 2.19%, p=0.041) and leg (+1.36 ± 1.87%, p=0.045) levels. The 3D analyses unveiled a length-dependent gradient in FF, ranging from 22.61 ±10.17% to 26.17 ± 10.79% at leg level. There was noticeable variance in longitudinal changes between muscles: +3.17 ± 6.86% (p=0.028) in the tibialis anterior compared to 0.37 ±4.97% (p=0.893) in the gastrocnemius medialis. MTR across the entire thigh volume showed a significant decline between the two time-points: -2.75 ± 6.58 (p=0.049), while no significant differences were noted for the 3D muscle volume and PD. No longitudinal changes were observed in any nerve metric. Potent correlations were identified between FF and primary clinical measures: CMTNSv2 (rho=0.656; p=0.001) and MRC in the lower limbs (rho=-0.877; p<0.001).

Discussion: Our results further support that qMRI is a promising tool for following up longitudinal changes in CMT1A patients, FF being the paramount MRI metric for both thigh and leg regions. It's crucial to scrutinize the post-imaging data extraction methods considering that annual changes are minimal (around +1.5%). Given the varied FF distribution, the existence of a length-dependent gradient, and the differential fatty involution across muscles, 3D volume analysis appeared more suitable than single slice analysis.

INTRODUCTION

Charcot-Marie-Tooth disease (CMT), also referred to as hereditary motor sensory neuropathy (HMSN) is an inherited neuromuscular disorder with an estimated prevalence of 1 in 2500 (1). The predominant variant, CMT1A, is associated with PMP22 duplication, which represent over half of all CMT diagnoses (2).

As new clinical trials are emerging for inherited neuropathies (3), the significant challenge is related to the identification of sensitive biomarkers for effective longitudinal evaluation. In slowly progressive conditions such as CMT neuropathies, there is a notable gap in the discovery of biomarkers capable of gauging therapeutic impacts (4). Consequently, identifying and assessing sensitive outcome metrics is vital for the success of upcoming clinical trials (5).

In recent years, quantitative Magnetic Resonance Imaging (qMRI) has emerged as a technique of choice to monitor changes in the muscle and nerve tissues in patients with neuromuscular disorders. Various imaging metrics such as the intramuscular fat fraction (FF), muscle volume, and magnetization transfer ratio (MTR), have found applications (6). One particular study in CMT1A patients highlighted a modest (1.7%) yet significant progression in FF within calf muscles over a year. This led to the proposition of FF as a potential biomarker for tracking patient progress. It is noteworthy that this assessment was based on the analysis of a singular central slice (7, 8). Given the known length-dependence characteristic of the disease (9), a comprehensive 3D series might offer richer insights. This trait, combined with the subtle FF changes, prompts a reconsideration: should MRI evaluations for follow-up be based on a 3D analysis or a single slice in the lower limbs? A significant obstacle for 3D analysis is sourcing a dependable automated segmentation technique for individual muscles (10, 11).

Expanding the scope of analysis, one might wonder the potential role of quantitative neurography in identifying biomarkers indicative of disease progression. Notably, metrics such as nerve volume, proton density (PD), and magnetization transfer ratio (MTR) at the sciatic and tibial nerve levels have been observed to deviate significantly in CMT1A patients when compared to healthy controls (12,13). However, the specific longitudinal variations of these metrics remain largely unexplored.

This study intends to meld qMRI with a dedicated muscle segmentation method so as to evaluate 3D longitudinal changes in lower limb muscles and the sciatic and tibial nerves over a year. The overarching goal is to discern the most pertinent MRI biomarker for tracking disease progression in CMT1A patients and to weight the merits of 3D volume against single slice analyses.

PATIENTS AND METHODS

Patients and Clinical assessment

Adult patients with genetically confirmed CMT1A (PMP22 duplication) from the Reference Center for Neuromuscular Disease and ALS (Marseille-France) volunteered to participate in this study from May 2016 to March 2019.

All participants had no history of other neuromuscular disorders and biological tests were performed to exclude any other conditions responsible for peripheral neuropathy.

Patients were clinically assessed twice within a 12-month interval, at baseline (T0) and one year later (T1), using demographic data, neurological examination and medical history. The Medical Research Council (MRC) scale (14) was used to assess muscle strength in the lower limbs. The MRC total score in the lower limbs (/60) was calculated taking into account six muscle groups on both sides i.e., quadriceps, ilio-psoas, gluteus maximus, hamstrings muscles, tibialis anterior and gastrocnemius muscle for the lower limbs.

Disease severity was assessed using several scores namely the Charcot Marie Tooth neurological score (CMTNSv2) (15), the Charcot Marie Tooth examination score (CMTES) and the overall neuropathy limitation scale (ONLS) (16). CMTNSv2 score is a composite score combining symptoms, signs and electrophysiological assessment. CMTES is another clinical score that does not take into account the electrophysiological testing. The ONLS was used to assess the functional disability in daily life. Two additional subscores were used i.e. CMTES LL and CMTES motor LL representing the lower limbs subscore and the lower limbs subscore motor items. ONLS LL refers to the lower limbs ONLS.

MRI protocol

Patients were positioned supine while the leg and thigh of the non-dominant limb were imaged using a combination of flexible coils on the top and spine coils integrated into the scanner bed.

After a localizer, sets of images were recorded in the axial plane at 1.5T (MAGNETOM Avanto, Siemens Healthineers, Erlangen, Germany) during approximately 45 minutes. Anatomical and quantitative imaging sequences were used in order to compute Fat Fraction (FF), Magnetisation Transfer Ratio and T2 maps. The corresponding parameters are summarized in Appendix 1.

As previously described (17, 18) the 3D gradient echo multi- echo dataset was used to generate FF maps, while the MTR map was computed from the normalized ratio of an image acquired with and without saturation and after correction for B1 field inhomogeneities (19).

Muscles and Nerves segmentation

Individual muscles segmentation was performed using a semi-automated propagation method based on a combination of diffeomorphic registration methods as previously described (11), (Figure 1). Briefly, individual muscles were manually segmented in 20% of the T1-weigthed axial slices and the corresponding masks were used for an automatic propagation along the muscle volume. The corresponding ROIs are described in Figure 2. Nerves delineation was performed entirely manually from GRE images, as shown in Figure 1. ROIs included both branches of the sciatic nerve (peroneal and tibial) in the distal part of the thigh. Manual

segmentations were performed in a blinded situation by two operators (E.F., C.P.M.) with more than 5 years of experience and double-checked by another experienced observer (M.-A.H). All slices were re-read together by the three operators in a single session after semi-automated propagation and a consensus was reached on corrections before extracting the quantitative metrics.

For anatomical standardization purposes among individuals, 18 slices were selected at the thigh level for the FF and MTR maps. The proximal limit selected for the thigh was the appearance of the short head of the biceps femoris. At the leg level, 20 slices were selected so that the distal limit of the region of interest was the disappearance of the gastrocnemius medialis. Quantitative measurements were computed for each muscle and averaged for each slice over the same area of interest for each subject.

Segmented masks were then resampled and registered to the quantitative MRI maps (FF, MTR, T2) and the mean values within each ROI and each slice were computed.

Two main analyses were performed to assess the most relevant ROI: one regarding the 3 central slices of the leg and the thigh, and one including the whole 3D volume. The human time required for each step was calculated to assess the cost-effectiveness of the two techniques.

Statistical analyses

Statistical analyses were performed using RStudio (19). Given the non-Gaussian distribution of the data, comparative analyses were performed using nonparametric Wilcoxon tests. The Spearman rank correlation (r) was used in order to assess the correlations between metrics. Differences were considered as statistically significant for p values lower than 0.05. Results are presented as means ± SD.

Data Availability Statement

All anonymized datasets and related documentation from this study are available upon request to qualified investigators, subject to a standard data sharing agreement.

Standard Protocol Approvals, Registrations, and Patient Consents

This research received no specific grant from any funding agency. Informed consent was obtained from all participants and the study was approved by the local ethics committee (IRB #2015-A00799-40).

RESULTS

Demographic and clinical data

Twenty-four CMT1A patients with PMP22 confirmed genetic diagnosis (mean age 51.9 ± 12.2 years; 7 females) were included in this study. Two patients were excluded due to incomplete data or technical problems. Follow-up and complete data extraction were therefore possible in twenty-two patients.

Initial clinical and demographic data of the remaining 22 CMT1A patients are presented in Table 1, along with the follow-up clinical evaluation. The mean follow-up interval was 12.3 months. CMT1A patients presented the classical phenotype with a length-dependent sensorimotor neuropathy, distal muscle weakness and predominant deformities in the lower limbs. Over a one-year period, none of the clinical scores did significantly change while muscle testing also remained unchanged (Table 1).

MRI muscle metrics at baseline (T0) and follow-up (T1)

MRI metrics included PD, FF, MTR, and muscle volume.

The 3D volume analysis showed that overall thigh muscles FF (T-All) was 7.13 ± 3.60% while the overall leg muscles FF (L-All) was much higher i.e. 20.06 ± 10.13 %.

At the thigh level, FF ranged from 5.62 ± 3.57% in the Rectus Femoris (RF) to 12.99 ± 7.7% in the Sartorius (Sa). At the leg level, FF ranged from 15.6 ± 12.93% in the deep posterior compartment to 29.85 ± 11.05% in the Gastrocnemius Medialis (GM). (Table 2B). 3D mean FF values computed at baseline for each muscle are displayed in Figure 2.

Detailed results for the FF, PD, MTR and volume analyses are shown in Table 2 and Table 3 respectively for the 3D volume and the central slices analyses.

MRI muscle metrics longitudinal changes (T1-T0)

- 3D Volume analysis (Table 2)

At the thigh level, a smaller but significant FF increase was also measured for the overall thigh muscles analysis: +1.04 ± 2.19% (p=0.041). Five muscles showed a slight but significant FF increase i.e. +1.28 ± 2.41% for the Biceps Femoris (BF) (p=0.021), +1.08 ± 2.62% for the Gracilis (Gr) (p=0.033), +1.45 ± 2.81% for the Rectus Femoris (RF) (p=0.037), + 0.39 ± 1.94% for the Semi Tendinosus (ST) (p=0.018) and +0.13 ± 2.61% for the Vastus Lateralis (VL) (p=0.046). At the leg level, a significant increase was found for the L-All FF: +1.36 ± 1.87% (p=0.045) while the tibialis anterior (TA) was the only muscle showing a significant FF increase i.e. +3.17 ± 3.86% (p=0.028).

Regarding the other metrics, there was a significant decrease in the overall thigh muscle analysis (MTR T-All): -2.75 ± 4.58 (p=0.049), with a significant MTR decrease in two muscles i.e RF (-3.6 ± 6.4 (p=0.004)) and the VL (-2.86 ± 6.27 (p=0.042)). MTR in the TA also showed a significant decrease over one year (-1.55 ± 3.32 (p=0.049)).

With respect to the thigh muscle volume, only the VL showed a significant longitudinal volume waste: -1.81 ± 5.41cm3 (p=0.042). No significant change was found for the PD metric.

- Central slices analysis (Table 3)

As compared to the 3D volume analysis, similar results were observed, and slight longitudinal differences were identified. More specifically, at the thigh level, the whole muscle analysis indicated a significant increase i.e. +1.11 ± 1.87% (p=0.041). Four muscles showed a FF increase ie. +1.09 ± 2.07% for the Biceps Femoris (BF) (p=0.011), Gr (+2.44 ± 3.72% (p=0.031)), ST (+ 0.96 ± 1.34% (p=0.038)) and VL (+1.78 ± 3.17% (p=0.007)).

At the leg level, a significant FF increase was also found for the overall leg muscles:.+1.54 ± 2.12% (p=0.032). Only the TA showed individual significant changes in FF +3.77 ± 3.09% (p=0.027).

Regarding the other metrics, there was a significant decrease in MTR in two muscles i.e. TA (-2.18 ± 4.65% (p=0.049)) and VL (-2.25 ± 5.04 % (p=0.041)) while MTR T-All did not change significantly (2.47 ± 6.93 (p=0.125).

No changes were found for PD and Volume analyses.

Cost-effectiveness of manual and semi-automated techniques

Segmentation of a single slice by a trained operator took around 10 minutes. For 3D volume analysis, five slices had to be segmented before the semi-automated propagation (50 minutes/patient). The propagation step was done in a single session for all patients. The process was automated and took around 15 minutes per patient. Although this process was automatic, a manual supervision (10 minutes/patient) was needed afterwards to correct the eventual errors brought by the propagation. Quantitative metrics were then extracted in a single time for the whole dataset (5 minutes).

Total processing time for 3D analysis of one patient was therefore estimated at 65 minutes. Considering only the 3 central slices instead of the entire volume, the processing would still have needed around 35 minutes. In comparison, analysis of the whole 3D volume with a fully manual segmentation approach would have taken around 200 minutes for each patient. The whole process was repeated twice (T0 and T1).

FF gradient

In order to identify whether longitudinal differences in FF were similar across the whole muscle volume, we divided the 3D muscle volume into 5 regions, each corresponding to 3 segmented slices as shown in Figure 4. Along the 3D volume at baseline, we observed a progressive increase in FF in the lower limbs ranging from 8.16 ± 3.86% to 9.0 ± 3.87% at the thigh level, and from 22.61 ± 10.17% to 26.17 ± 10.79% at the leg level.

Analysis by regions showed that the difference in overall FF was more pronounced in the central parts of both the leg and the thigh (Region 2, corresponding to the central slices analysis). At this level, a maximum significant difference was observed i.e. +1.37 ± 3.25% (p=0.038) for the thigh and +1.69 ± 3.07% (p=0.026) for the leg.

Longitudinal assessment of nerves metrics

Sciatic nerve at the thigh level and tibial nerve at the leg level were clearly identified in the 3D-GRE images so that segmentation of such small structures was possible and longitudinal progression of multiple metrics i.e. PD, MTR, T2 and nerve Volume was performed.

Detailed results are available in the Appendix 2 and showed no significant longitudinal difference for any nerve metric between baseline and follow-up evaluation.

Clinical correlations

Clinical correlations with MRI metrics are reported in the heatmap (Figure 4A). Strong correlations were found between FF and the most relevant clinical scores.
Central slices FF was correlated with CMTNSv2 (rho=0,656; p=0,001) and inversely correlated with MRC testing in the lower limb (rho=-0.877; p<0,001).
FF in the TA was also correlated with CMTNSv2 (rho=0,605; p=0,004).
Among the other analyzed metrics, MTR in the whole thigh was inversely correlated with CMTNSv2 (rho=-0,608; p=0,002).

DISCUSSION

In the present study, we quantitatively and longitudinally investigated different lower limbs muscles and nerves MRI metrics in CMT1A patients over a year period. We used a quantitative imaging pipeline already developed in previous studies (10, 18, 21) for which quantitative MRI was combined to a semi-automated segmentation method of individual muscles, allowing us to analyses both the central slices and a global 3D volume. We mainly found a significant increase in overall FF of the leg for the 3D volume analysis: +1.36 ± 1.87% (p=0.045) and confirmed a similar increase (+1.54 ± 2.12%, p=0.032) in the central region of the leg. Our results confirm in an independent cohort the main findings previously published by Morrow et al., i.e a progression of around 1.5% of FF in the leg over 1 year in CMT1A patients, detected in a single central slice analysis (7,8).
Of interest, 3D volume and central slices analyses also indicated in our cohort a FF increase at the thigh level respectively +1.04 ± 2.19% p=0.041 and +1.11 ± 1.87% (p=0.041) which has not been described in previous studies.
As FF progression was roughly similar between central slices and 3D volume analyses, the usefulness of a 3D approach can be questioned and one might suggest that a central region analysis should be preferred for clinical trials due to the time consumption and the complexity of the 3D volume analysis. In fact, segmentation of the 3D volume of interest was made possible thanks to a semi-automated propagation segmentation tool (10) that allowed us to analyze a larger muscle volume without a massive increase in work time while providing more robust statistical results thanks to a larger amount of analyzed data. Moreover, this 3D analysis showed important additional informations regarding the fatty replacement. We showed here that longitudinal FF changes were not exactly homogeneous along the whole muscle volume and confirmed the length-dependent gradient of FF we previously reported in the lower limbs of CMTA patients (9). This FF gradient and the heterogeneity of FF infiltration across different muscles have to be taken into account in quantitative muscle MRI studies of CMT patients. As a matter of example, the tibialis anterior would be the most interesting muscle to follow up given its larger FF progression i.e. 3%. This non-uniformity in

fat replacement is not specific to CMT1A patients and has been described in other neuromuscular pathologies such as the Duchenne muscular dystrophy (22).

Our results are also supportive of the fact that FF would be the most relevant biomarker for the follow-up of the disease progression in CMT1A. We also identified the overall muscle MTR computed from the 3D dataset at the thigh level as another metric of interest for the longitudinal analysis. A muscle MTR decrease has been previously reported in several muscular pathologies (21, 23, 24) and could reflect changes in muscle molecular composition that may precede fatty muscle involution. This result will have to be confirmed in further studies and a better understanding of the histological counterpart of MTR changes is warranted.

Regarding the nerve analyzes, no significant difference was observed over a year period. Of interest, in CMT1A patients, multiple biomarkers abnormalities have been identified as compared to healthy controls. Morphological changes regarding nerve volume (12) or cross-sectional diameter (25) have been described in line with the anatomical long-term demyelination and remyelination process leading to a thickening of peripheral nerves. An increased PD (12) and a decrease in MTR (12, 13) of the sciatic nerve have also been reported. So far, changes of these abnormalities over time were unknown in CMT1A patients. Our results clearly indicate that none of the qMRI metrics selected (PD, MTR, T2 and volume) is changing over a 1-year period of time in our cohort. This lack of variation could be partly explained by the technical difficulties associated with the very small nerve ROI, corresponding to just a few pixels. The extraction of quantitative metrics in such small ROIs is always difficult inasmuch as for longitudinal studies registration between images recorded at different time-points should be perfect. Further studies with higher images resolution might be of interest (26). On the contrary to the qMRI metrics, the clinical scores analyzed in our study did not change significantly over this short period of time. These scores suffer from the ceiling or floor effects described in clinical trials in CMT1A patients (4, 5, 27). Interestingly, as previously described (7, 8, 22), FF was well correlated with the main clinical scores or with lower limb testing further supporting FF as a relevant biomarker for assessing disease severity in CMT1A patients.

One has to keep in mind that qMRI results strongly rely on sophisticated acquisition and post-processing methods which must be scrutinized in terms of robustness. One of the difficulties in implementing large volume analyses is the time needed to manually annotate a large number of images. In the present study, we were able to spare time using a semi-automated segmentation method enabling to conduct a larger 3D muscle volume analysis. Therefore, in a fully manual approach, if automated or semi-automated propagation tools are not available, the analysis of the central slices can be preferred to spare some time on manual segmentation. However, with the help of these tools, already deployed in other centers (28), the time required for 3D analysis is only slightly longer than the one necessary for single slice analysis, and enables us to study a more representative muscle volume. In that context, artificial intelligence-based segmentation methods will definitely be an important step towards standardizing and optimizing these techniques, as well as their implementation in therapeutic trials (11, 29, 30).

In conclusion, this study highlights quantitative MRI as a technique of interest for assessing disease severity and progression in CMT1A patients. More specifically, FF, which reflects the

fibro-adipotic process occurring in neuropathies appears as the most interesting metric for longitudinal studies with a yearly progression rate of +1.5%. A particular attention must be paid to the post-processing pipelines used for data extraction, especially in this pathology where changes over a one-year period are very small. The heterogeneity of FF distribution, the presence of a length-dependent gradient and the variability of fatty involution from one muscle to another, argue in favor of a 3D volume analysis which will definitely be possible with currently developed segmentation methods based on artificial intelligence. Such a progress should be of high interest for coming clinical trials.

TABLES

Table 1: Demographic and clinical data at baseline and follow-up evaluation in CMT1A patients

	CMT1A baseline	CMT1A follow-up	p
Sex (F/M)	22 (15/7)	22 (15/7)	/
Age	46.5 ± 15.8	47.6 ± 15.8	/
Disease duration	27.2 ± 18.6	28.2 ± 18.7	/
CMTNSv2	15.2 ± 5.9	15.7 ± 6.0	*0.88*
CMTES	10.4 ± 4.2	10.5 ± 4.1	*0.85*
CMTES LL	7.5 ± 3.4	8.04 ± 3.0	*0.57*
CMTES motor LL	3.7 ± 1.7	3.7 ± 1.7	*0.65*
ONLS LL	1.7 ± 0.9	1.7 ± 0.6	*0.77*
ONLS total	3.5 ± 1.2	3.6 ± 1.2	*0.80*
MRC LL (/60)	49.0 ± 18.4	48.3 ± 19.1	*0.80*
MRC TA	3.4 ± 1.3	3.4 ± 1.5	*0.55*

Shown as mean ± SD
Abbreviations:
CMT1A: Charcot Marie Tooth type 1A
CMTNSvs2: Charcot Marie Tooth Neuropathy Score version 2
CMTES: Charcot Marie Tooth examination score
CMTES LL: Charcot Marie Tooth examination score (lower limb subpart)
CMTES motor LL: Charcot Marie Tooth examination score (motor lower limb subpart)
ONLS total: Overall neuropathy limitation scale
ONLS LL: Overall neuropathy limitation scale (Lower limb subpart)
MRC score: Medical research council score
TA: Tibialis Anterior

401 **Table 2: Longitudinal changes in 3D volume MRI muscle metrics between baseline (T0) and one-year later (T1)**

402

	METRIC	FF (%)		MTR		PD		Volume	
Section		T0	T1	T0	T1	T0	T1	T0	T1
LEG	TA	***24.39 ± 7.57****	***27.56 ± 7.45****	***36.52 ± 12.97****	***34.97 ± 13.63****	685.98 ± 188.24	749.96 ± 184.75	59.45 ± 20.98	57.98 ± 21.24
	DPC	15.6 ± 12.93	15.59 ± 12.99	40.45 ± 9.26	40.13 ± 11.06	620.59 ± 174.84	663.87 ± 157.97	45.02 ± 16.49	43.96 ± 14.26
	GL	24.05 ± 11.86	23.69 ± 11.63	36.8 ± 14.98	37.27 ± 14.22	751.92 ± 278.2	822.15 ± 266.16	25.04 ± 19.92	24.93 ± 17.19
	GM	29.85 ± 11.05	31.61 ± 9.88	30.0 ± 14.56	29.73 ± 14.67	829.43 ± 200.44	870.79 ± 287.04	47.56 ± 31.82	48.57 ± 31.29
	LC	29.29 ± 10.96	30.82 ± 20.66	33.39 ± 15.31	32.79 ± 15.35	756.28 ± 260.77	838.08 ± 197.32	41.92 ± 16.78	42.31 ± 16.15
	So	15.77 ± 8.2	16.44 ± 8.15	41.87 ± 12.53	41.19 ± 12.94	670.08 ± 226.78	738.79 ± 236.51	168.65 ± 61.91	164.56 ± 59.64
	L-All	***20.06 ± 10.13****	***21.42 ± 10.15****	38.72 ± 11.43	37.84 ± 12.37	696.81 ± 203.11	759.27 ± 203.36	387.17 ± 147.67	379.79 ± 140.0
THIGH	Ad	7.11 ± 2.91	7.47 ± 2.82	49.46 ± 2.14	47.06 ± 6.8	500.71 ± 98.94	501.85 ± 106.33	190.9 ± 74.77	189.39 ± 70.57
	BF	***7.42 ± 2.39****	***8.45 ± 2.84****	48.37 ± 1.68	45.87 ± 6.67	553.27 ± 99.13	583.28 ± 127.66	117.72 ± 43.06	117.05 ± 40.82
	Gr	***9.32 ± 3.44****	***10.98 ± 4.79****	47.4 ± 2.51	44.72 ± 8.47	535.31 ± 134.2	579.76 ± 164.96	29.45 ± 11.84	28.43 ± 9.86
	RF	***5.90 ± 3.66****	***7.3 ± 5.26****	***48.96 ± 2.76****	***45.76 ± 7.27****	560.48 ± 105.04	604.58 ± 172.81	34.21 ± 14.93	33.43 ± 13.95
	SM	9.83 ± 4.55	11.14 ± 8.16	46.71 ± 7.01	45.45 ± 7.30	592.36 ± 139.31	604.26 ± 141.58	67.81 ± 22.09	70.3 ± 19.51
	ST	***8.12 ± 3.22****	***8.46 ± 3.19****	48.85 ± 2.09	46.36 ± 7.15	554.31 ± 121.52	572.07 ± 128.67	63.22 ± 22.81	61.54 ± 22.24
	Sa	12.99 ± 7.7	13.45 ± 6.07	45.05 ± 6.39	42.87 ± 8.49	564.07 ± 122.78	584.27 ± 127.3	30.04 ± 10.54	29.33 ± 9.39
	VI	5.62 ± 3.57	6.15 ± 4.6	49.78 ± 2.27	47.36 ± 7.05	600.48 ± 164.54	565.01 ± 90.35	142.01 ± 54.64	139.66 ± 51.39
	VL	***7.45 ± 6.92****	***7.58 ± 4.48****	48.21 ± 4.24	46.31 ± 6.75	634.24 ± 108.21	634.24 ± 108.21	***161.35 ± 53.95****	***159.68 ± 49.71****
	VM	4.91 ± 2.29	5.48 ± 2.96	49.84 ± 1.71	47.62 ± 6.86	546.69 ± 85.65	555.85 ± 103.74	123.55 ± 41.89	123.05 ± 42.62
	T-All	***7.13 ± 3.60****	***8.27 ± 3.25****	***48.84 ± 2.4****	***46.57 ± 6.9****	562.4 ± 81.19	567.5 ± 93.85	960.28 ± 309.11	952.87 ± 293.22

403

Formatted: Numbering: Continuous

Shown as mean ± SD

*indicates significant differences between T0 and T1 (in bold + italics)

Abbreviations: Ad= Adductor. BF= Biceps Femoris. DPC = Deep Posterior Compartment. GL = Gastrocnemius Lateralis. GM= Gastrocnemius Medialis. Gr=Gracilis. L-All= Leg All. LC= Lateral Compartment. MTR= Magnetiszation Transfert Ratio. PD = Proton Density. RF= Rectus Femoris. Sa= Sartorius. SM = Semi Membranosus. So = Soleus. ST= Semi Tendinosus. TA= Tibialis anterior. VI= Vastus Intermedius. VL = Vastus Lateralis. VM = Vastus Medialis.

411 **Table 3: Longitudinal changes in central slices MRI muscle metrics between baseline (T0) and one-year later (T1)**

412

	METRIC	FF (%)		MTR		PD		Volume	
Section		T0	T1	T0	T1	T0	T1	T0	T1
LEG	TA	***24.12 ± 7.90****	***27.89 ± 8.92****	36.99 ± 13.32	34.81 ± 14.81	715.48 ± 205.12	769.40 ± 205.32	6.26 ± 1.68	6.41 ± 2.08
	DPC	15.39 ± 12.69	15.82 ± 13.14	40.50 ± 9.31	39.81 ± 11.33	627.46 ± 179.43	668.37 ± 171.06	5.32 ± 1.46	4.96 ± 1.33
	GL	23.92 ± 11.74	23.40 ± 12.76	35.96 ±14.02	36.44 ± 15.18	726.98± 286.25	850.56 ± 281.68	3.76 ± 2.86	4.22 ±2.45
	GM	***30.51 ± 11.65****	***32.76 ± 10.51****	28.45 ± 15.59	28.19 ± 15.42	878.36± 229.04	899.39 ± 287.82	4.26 ± 4.18	4.75 ± 4.06
	LC	29.21 ± 11.29	31.23 ± 12.36	32.82 ± 15.59	32.67 ± 16.62	796.89 ± 285.57	869.69 ± 210.80	4.43 ± 1.81	4.46 ± 2.12
	So	15.04 ± 7.65	16.49 ± 8.51	41.95 ± 12.36	40.84 ± 13.02	680.80 ± 228.91	748.61 ± 245.06	18.38 ± 5.02	18.12 ± 5.78
	L-All	***20.05 ± 10.08****	***21.60 ± 10.53****	38.32 ± 11.43	37.49 ± 12.71	715.13 ± 210.17	773.22 ± 213.08	40.92 ± 13.60	41.01 ± 15.3
THIGH	Ad	6.43 ± 2.18	7.42 ± 3.89	49.51 ± 1.62	46.97 ± 7.92	522.86 ± 107.88	550.40 ± 105.36	13.87 ± 11.20	13.67 ± 11.19
	BF	***7.21 ± 2.69****	***8.30 ± 3.25****	48.23 ±2.41	45.88 ± 6.87	552.86 ± 107.88	601.09 ± 136.65	10.36 ± 3.66	9.90 ± 3.88
	Gr	***8.88 ± 4.04****	***11.32 ± 6.19****	47.43 ± 3.30	44.21 ± 9.19	554.63 ± 101.41	562.55 ± 146.83	2.35 ± 0.99	2.33 ± 0.85
	RF	4.85 ±3.73	7.83 ± 7.89	48.85 ± 3.21	45.44 ± 9.05	592.19 ± 172.92	618.92 ± 128.91	2.38 ± 2.06	2.24 ± 1.93
	SM	8.88 ± 4.67	10.08 ± 5.75	47.75 ± 3.19	45.10 ± 7.77	590.11 ± 136.70	609.98 ± 178.91	7.13 ± 3.74	6.92 ± 3.50
	ST	***7.85 ± 2.73***	***8.81 ± 3.43****	48.65 ± 2.50	46.32 ± 7.54	577.72 ± 126.08	588.49 ± 137.63	5.10 ± 2.3	4.93 ± 2.10
	Sa	11.93 ± 5.67	14.06 ± 6.15	46.06 ± 4.28	42.52 ± 9.03	571.25 ± 131.12	571.25 ± 131.12	2.66 ± 0.80	2.58 ± 0.64
	VI	4.62 ± 2.45	5.04 ± 2.97	49.94 ±1.89	47.73 ± 7.00	556.41 ± 130.25	598.48 ± 99.98	11.53 ± 3.33	11.45 ±3.88
	VL	***5.45 ± 2.66****	***7.23 ± 4.74****	***48.91 ± 2.20****	***46.24 ±7.13****	***620.47 ± 179.45****	***675.13 ± 122.82****	12.54 ± 5.01	12.43 ± 4.73
	VM	4.63 ± 2.01	5.17 ± 2.69	49.68 ± 2.57	47.57 ± 6.98	552.80 ± 97.08	559.34 ± 96.25	11.91 ± 5.01	11.43 ± 4.73
	T-All	***6.10 ± 2.15****	***7.21 ± 3.38****	49.11 ±1.82	47.57 ± 6.98	568.71 ± 107.09	593.33 ± 89.45	78.60 ± 22.01	78.16 ± 22.75

Shown as mean ± SD

*indicates significant differences between T0 and T1 (in bold + italics)

Abbreviations: Ad= Adductor. BF= Biceps Femoris. DPC = Deep Posterior Compartment. GL = Gastrocnemius Lateralis. GM= Gastrocnemius Medialis. Gr=Gracilis. L-All= Leg All. LC= Lateral Compartment. MTR= Magnetiszation Transfert Ratio. PD = Proton Density. RF= Rectus Femoris. Sa= Sartorius. SM = Semi Membranosus. So = Soleus. ST= Semi Tendinosus. TA= Tibialis anterior. VI= Vastus Intermedius. VL = Vastus Lateralis. VM = Vastus Medialis.

Figure Legends:

Figure 1: Imaging Pipeline

Schematic representation of the complete imaging pipeline used to extract quantitative MRI data. After MRI acquisition, muscle from 5 initial slices were manually segmented. Then a semi-automated segmentation propagation technique was used to extend the segmentation through the entire muscle volume. Sciatic and tibial nerves nerves were completely manually segmented from 3D-GRE sequence. The masks obtained were then projected onto quantitative MRI maps to obtain the various metrics: 3D Volume, Proton Dentity (PD), Magnetization Transfer Ratio (MTR) and T2.

Figure 2: Detailed segmented ROI and Individual muscle FF at baseline with the 3D analysis

A. Example of T1W axial images from a CMT1A patient left limb: thigh (upper panel) and leg (lower panel) at baseline are shown in the left side, and follow-up evaluation in the right side. All individual regions of interest were drawn in color using FSLeyes software with eleven regions at thigh levels and six regions at leg level.
B. Box and whisker plots of muscle fat fraction for each individual muscle obtain at baseline with the 3D analysis. Box-and whiskers represent median, Interquartile and range with outliers identified with a dot. Mean FF ranged from 5.62% (Rectus Femoris) to 12.99% (Sartorius) at thigh level and from 15.6% (Deep posterior compartment) to 29.85% at leg level (gastrocnemius medalis).

Abbreviations: Ad= Adductor, BF= Biceps Femoris, DPC= Deep posterior compartment, FF= Fat Fraction, L-All = Leg All, LC= Lateral Compartment, GL= Gastrocnemius Lateralis, GM= Gastrocnemius Medialis, Gr=Gracilis, RF= Rectus Femoris, Sa= Sartorius, SM = Semi Membranosus, So= Soleus, ST= Semi Tendinosus, T-All= Thigh All, TA= Tibialis Anterior, VI= Vastus Intermedialis, VL= Vastus lateralis, VM = Vastus Medialis

Figure 3: FF length-dependent gradient with 3D volume analysis

Example of a CMT1A patient sagittal and axial T1W slices at thigh and leg level, with all segmented ROI from the FSLeyes software (each color represents a different region). The whole 3D volume was then divided into 5 regions (3 slices each) to assess the FF variation along the limb.

The graph shows the progression of FF from region 0 (proximal part of the limb) to region 4 (distal part) at baseline (T0) (blue curve) and Follow-Up (T1) (orange curve). Maximal longitudinal variation between T0 and T1 was seen in the central part of both thigh and leg levels (region 2).

Formatted: Numbering: Continuous

Figure 4: Heatmap and correlation curves between MRI metrics and clinical parameters at baseline

•A: Heatmap of the correlations between the main clinical scores and the most relevant metrics that showed significant longitudinal differences.

•B: CMTNSv2 was correlated with Overall FF (rho= 0.57, p=0.005), Overall FF at leg level (rho= 0.63, p=0.002) and Overall FF in region 2 at leg level (rho= 0.66, p=0.001).

Abbreviations: Ad= Adductor, BF= Biceps Femoris, CMTES: Charcot Marie Tooth examination score, CMTES LL: Charcot Marie Tooth examination score (lower limb subpart) CMTES motor LL: Charcot Marie Tooth examination score (motor lower limb subpart), CMTNSvs2: Charcot Marie Tooth Neuropathy Score v2, FF= Fat Fraction, MTR= Magnetiszation Transfert Ratio, MRC score: Medical research council score, ONLS total: Overall neuropathy limitation scale, ONLS LL: Overall neuropathy limitation scale (Lower limb subpart), PD = Proton Density, SM = Semi Membranosus, ST= Semi Tendinosus, TA= Tibialis anterior, VM = Vastus Medialis

REFERENCES

1. Barreto LCLS, Oliveira FS, Nunes PS, et al. Epidemiologic Study of Charcot-Marie-Tooth Disease: A Systematic Review. Neuroepidemiology. 2016;46(3):157-65.

2. Fridman V, Bundy B, Reilly MM and al., Inherited Neuropathies Consortium. CMT subtypes and disease burden in patients enrolled in the Inherited Neuropathies Consortium natural history study: a cross-sectional analysis. J Neurol Neurosurg Psychiatry. 2015 Aug;86(8):873-8.

3. Morena J, Gupta A, Hoyle JC. Charcot-Marie-Tooth: From Molecules to Therapy. IJMS. 12 juill 2019;20(14):3419.

4. Rossor AM, Shy ME, Reilly MM. Are we prepared for clinical trials in Charcot-Marie-Tooth disease? Brain Research. feb 2020;1729:146625.

5. Gess B, Baets J, De Jonghe P, Reilly MM, Pareyson D, Young P. Ascorbic acid for the treatment of Charcot-Marie-Tooth disease. Ascorbic acid for the treatment of Charcot-Marie-Tooth disease. Cochrane Database Syst Rev. 2015 Dec 11;2015(12):CD011952

6. Chhabra A, Madhuranthakam AJ, Andreisek G. Magnetic resonance neurography: current perspectives and literature review. Eur Radiol. 2018 Feb;28(2):698-707.

7. Morrow JM, Sinclair CDJ, Fischmann A, et al. MRI biomarker assessment of neuromuscular disease progression: a prospective observational cohort study. Lancet Neurol. 2016 Jan;15(1):65-77.

8. Morrow JM, Evans MRB, Grider T, Sinclair CDJ, Thedens D, Shah S, Yousry TA, Hanna MG, Nopoulos P, Thornton JS, Shy ME, Reilly MM. Validation of MRC Centre MRI calf muscle fat fraction protocol as an outcome measure in CMT1A. Neurology. 2018 Sep 18;91(12):e1125-e1129.

9. Bas J, Ogier AC, Le Troter A, et al. Fat fraction distribution in lower limb muscles of patients with CMT1A: A quantitative MRI study. Neurology. 2020 Apr 7;94(14):e1480-e1487.

10. Ogier A, Sdika M, Foure A, Le Troter A, Bendahan D. Individual muscle segmentation in MR images: A 3D propagation through 2D non-linear registration approaches. Annu Int Conf IEEE Eng Med Biol Soc. 2017 Jul;2017:317-320.

11. Hostin MA, Ogier AC, Michel CP, Le Fur Y, Guye M, Attarian S, Fortanier E, Bellemare ME, Bendahan D. The Impact of Fatty Infiltration on MRI Segmentation of Lower Limb Muscles in Neuromuscular Diseases: A Comparative Study of Deep Learning Approaches. J Magn Reson Imaging. 2023 Apr 6.

514 12. Fortanier E, Ogier AC, Delmont E, et al. Quantitative assessment of sciatic nerve
515 changes in Charcot-Marie-Tooth type 1A patients using magnetic resonance
516 neurography. Eur J Neurol. 2020 Aug;27(8):1382-1389.

517 13. Dortch RD, Dethrage LM, Gore JC, Smith SA, Li J. Proximal nerve magnetization
518 transfer MRI relates to disability in Charcot-Marie-Tooth diseases. Neurology.
519 2014;83(17):1545-53.

520 14. Compston A. Aids to the investigation of peripheral nerve injuries. Medical Research
521 Council: Nerve Injuries Research Committee. His Majesty's Stationery Office: 1942; pp.
522 48 (iii) and 74 figures and 7 diagrams; with aids to the examination of the peripheral
523 nervous system. By Michael O'Brien for the Guarantors of Brain. Saunders Elsevier:
524 2010; pp. [8] 64 and 94 Figures. Brain. 2010 Oct;133(10):2838-44.

525 15. Murphy SM, Herrmann DN, McDermott MP, Scherer SS, Shy ME, Reilly MM, et al.
526 Reliability of the CMT neuropathy score (second version) in Charcot-Marie-Tooth
527 disease. Journal of the peripheral nervous system : JPNS. 2011;16(3):191-8

528 16. Graham RC, Hughes RA. A modified peripheral neuropathy scale: the Overall
529 Neuropathy Limitations Scale. Journal of neurology, neurosurgery, and psychiatry.
530 2006;77(8):973-6.17. Leporq B, Lambert SA, Ronot M, *et al.* Quantification of the
531 triglyceride fatty acid composition with 3.0 T MRI. *NMR Biomed* 2014;**27**:1211–21.

532 17. Leporq B, Lambert SA, Ronot M, *et al.* Quantification of the triglyceride fatty acid
533 composition with 3.0 T MRI. *NMR Biomed* 2014;**27**:1211–21. doi:10.1002/nbm.3175

534 18. Ansari B, Salort-Campana E, Ogier A, et al. Quantitative muscle MRI study of patients
535 with sporadic inclusion body myositis. Muscle Nerve. 2020;61(4):496-503.

536 19. Sinclair CDJ, Morrow JM, Hanna MG, et al. Correcting radio frequency inhomogeneity
537 effects in skeletal muscle magnetisation transfer maps: CORRECTION OF MUSCLE
538 MTR MAPS. NMR Biomed. 2012;25(2):262-270. doi:10.1002/nbm.1744.

539 20. RStudio Team (2020). RStudio: Integrated Development for R. RStudio, PBC, Boston,
540 MA URL.

541 21. Durelle C, Delmont E, Michel C, Trabelsi A, Hostin MA, Ogier A, Bendahan D, Attarian
542 S. Quantification of muscle involvement in familial amyloid polyneuropathy using MRI.
543 Eur J Neurol. 2023 Jul 9.

544 22. Hooijmans M, Niks E, Burakiewicz J, et al. Non-uniform muscle fat replacement along
545 the proximodistal axis in Duchenne muscular dystrophy. Neuromuscul Disord 2017;
546 27(5): 458-464.

547 23. Sinclair C, Morrow J, Miranda M, et al. Skeletal muscle MRI magnetisation transfer ratio
548 reflects clinical severity in peripheral neuropathies. J Neurol Neurosurg Psychiatry 2012;
549 83(1): 29-32

550 24. Laurent D, Riek J, Sinclair CDJ, Houston P, Roubenoff R, Papanicolaou DA, Nagy A,
551 Pieper S, Yousry TA, Hanna MG, Thornton JS, Machado PM. Longitudinal Changes in
552 MRI Muscle Morphometry and Composition in People With Inclusion Body Myositis.
553 Neurology. 2022 Aug 30;99(9):e865-e876.

554 25. Sinclair CDJ, Miranda MA, Cowley P, et al. MRI shows increased sciatic nerve cross
555 sectional area in inherited and inflammatory neuropathies. J Neurol Neurosurg
556 Psychiatry. 2011;82(11):1283-1286.

557 26. Sveinsson B, Rowe OE, Stockmann JP, Park DJ, Lally PJ, Rosen MS, Barry RL, Eichler
558 F, Rosen BR, Sadjadi R. Feasibility of simultaneous high-resolution anatomical and
559 quantitative magnetic resonance imaging of sciatic nerves in patients with Charcot-
560 Marie-Tooth type 1A (CMT1A) at 7T. Muscle Nerve. 2022 Aug;66(2):206-211. doi:
561 10.1002/mus.2764

562 27. Eichinger K, Sowden JE, Burns J, McDermott MP, Krischer J, Thornton J, Pareyson D,
563 Scherer SS, Shy ME, Reilly MM, Herrmann DN. Accelerate Clinical Trials in Charcot-
564 Marie-Tooth Disease (ACT-CMT): A Protocol to Address Clinical Trial Readiness in
565 CMT1A. Front Neurol. 2022 Jun 27;13:930435.

566 28. Heskamp L, Ogier A, Bendahan D, Heerschap A. Whole-muscle fat analysis identifies
567 distal muscle end as disease initiation site in facioscapulohumeral muscular dystrophy.
568 Commun Med (Lond). 2022 Dec 1;2(1):155. doi: 10.1038/s43856-022-00217-1. Erratum
569 in: Commun Med (Lond). 2023 Jan 12;3(1):6. PMID: 36450865; PMCID:
570 PMC9712512).

571 29. Ronneberger O, Fischer P, Brox T. U-net: Convolutional networks for biomedical image
572 segmentation. *Medical Image Computing and Computer-Assisted Intervention-MICCAI*
573 *2015: 18th International Conference*, Munich, Germany, October 5-9, 2015,
574 Proceedings, Part III 18:Springer; 2015. p 234-241.

575 30. Ding J, Cao P, Chang HC, Gao Y, Chan SHS, Vardhanabhuti V. Deep learning-based
576 thigh muscle segmentation for reproducible fat fraction quantification using fat–water
577 decomposition MRI. *Insights Imaging* 2020; 11(1): 1-11.

578

579

580

581

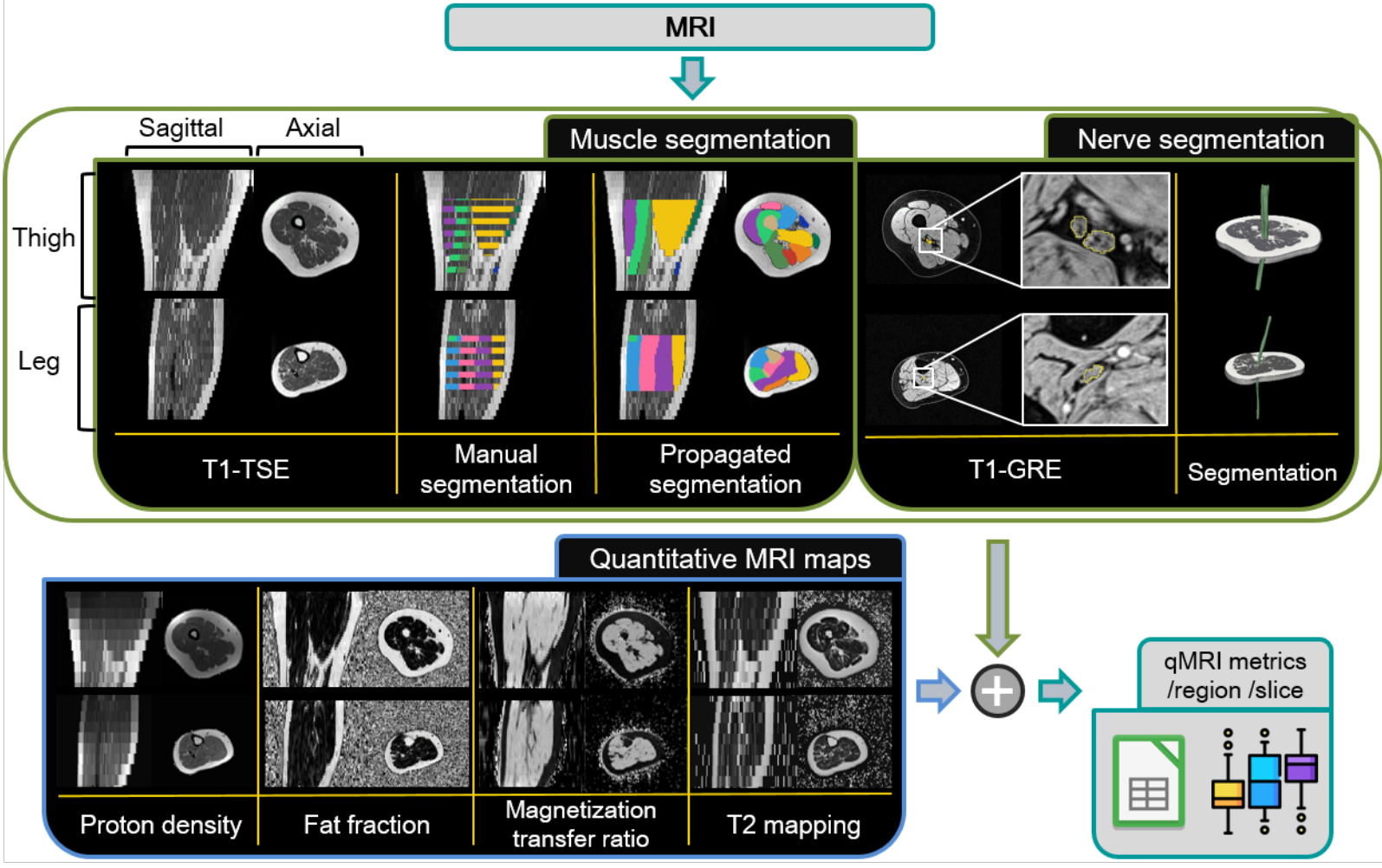
MRI
Sagittal
Axial
Muscle segmentation
Nerve segmentation
Thigh
Leg
T1-TSE
Manual segmentation
Propagated segmentation
T1-GRE
Segmentation
Quantitative MRI maps
Proton density
Fat fraction
Magnetization transfer ratio
T2 mapping
qMRI metrics /region /slice

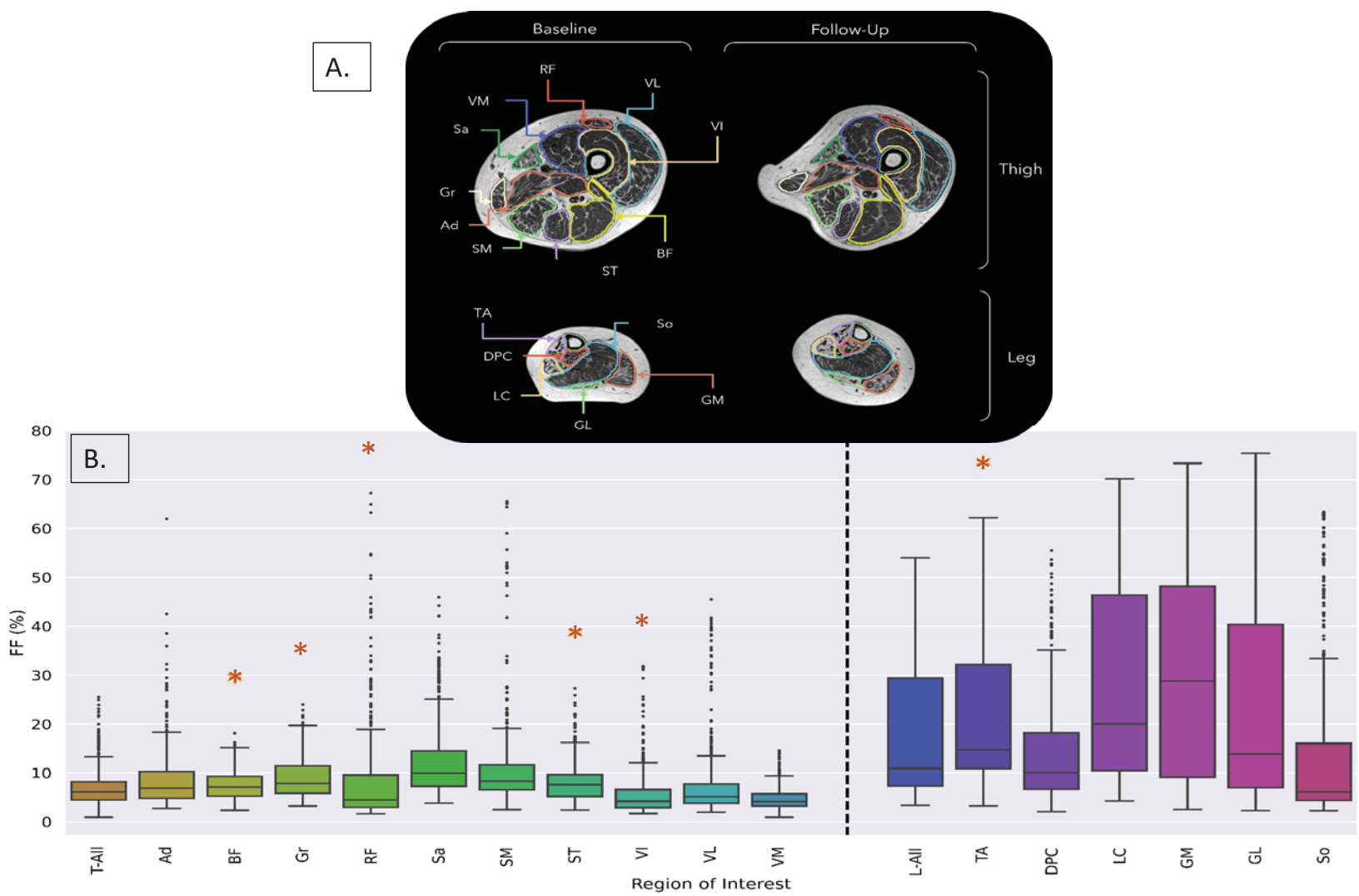
A.
Baseline
Follow-Up
RF
VL
VM
Sa
VI
Gr
Ad
SM
BF
ST
Thigh
TA
So
DPC
LC
GM
GL
Leg
B.
FF (%)
0
10
20
30
40
50
60
70
80
T-All
Ad
BF
Gr
RF
Sa
SM
ST
VI
VL
VM
L-All
TA
DPC
LC
GM
GL
So
Region of Interest

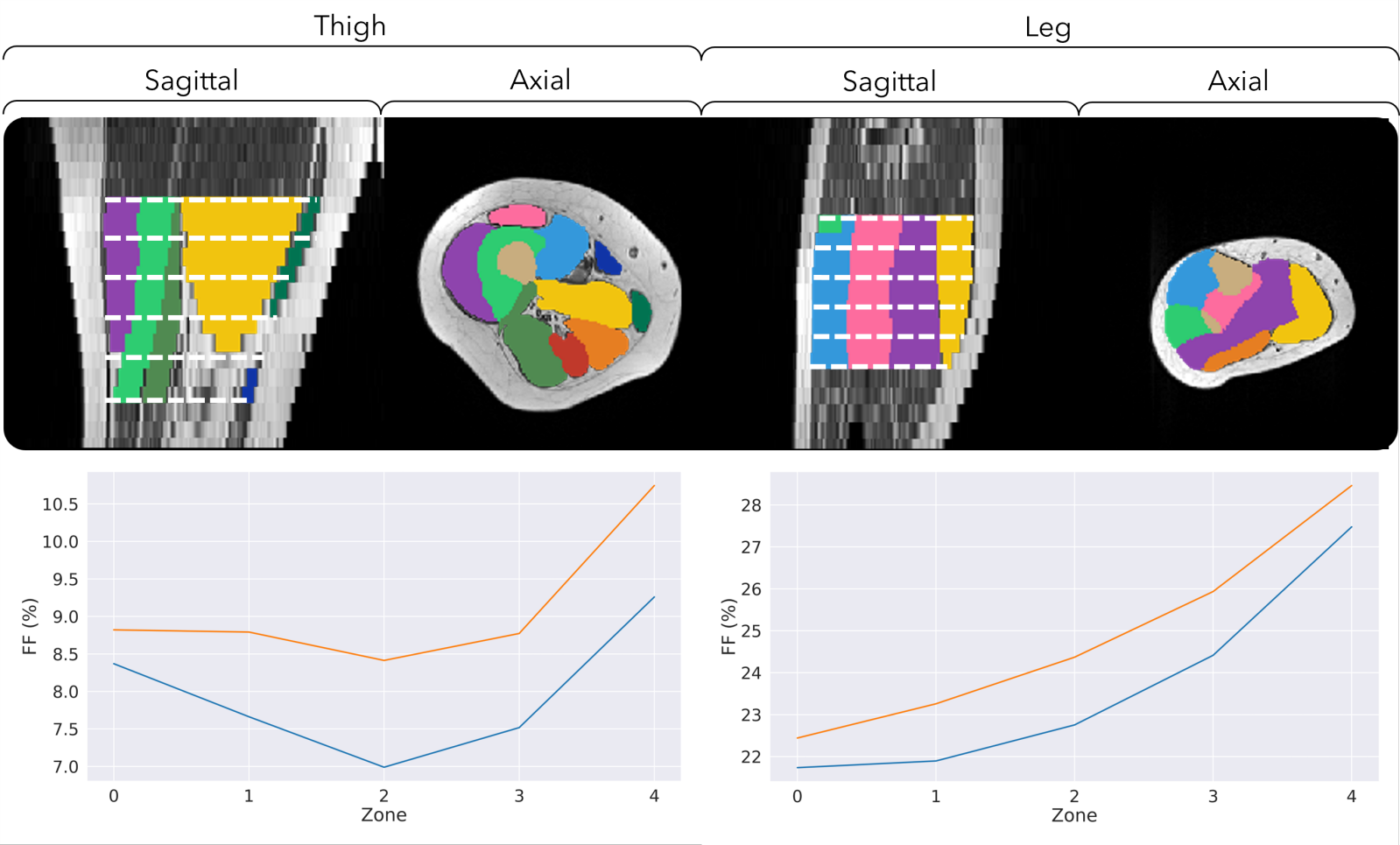
Thigh
Leg
Sagittal
Axial
Sagittal
Axial
FF (%)
Zone
FF (%)
Zone

A.

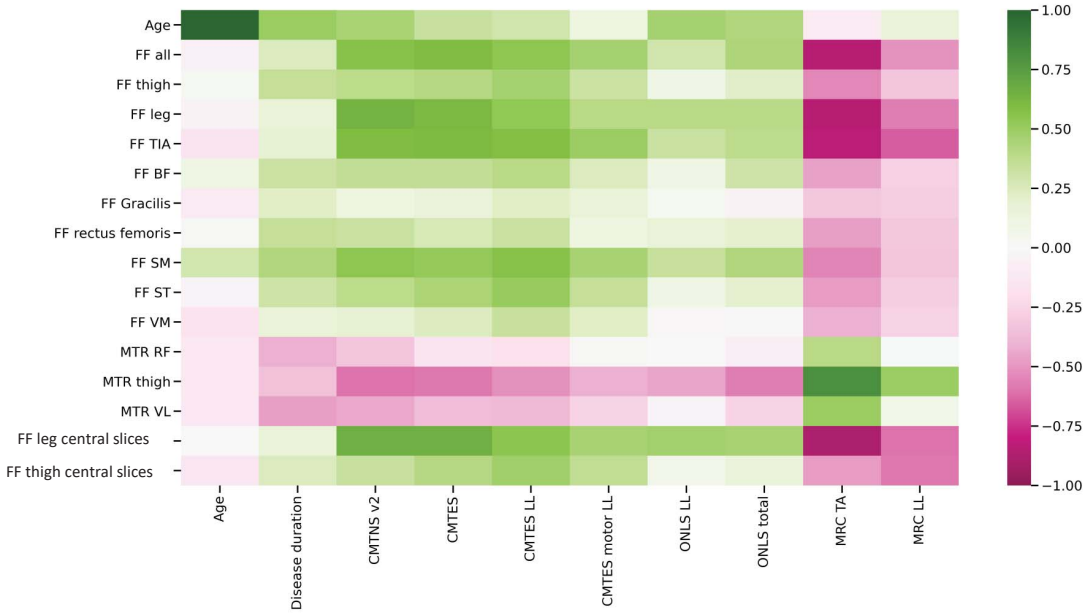
Age
FF all
FF thigh
FF leg
FF TIA
FF BF
FF Gracilis
FF rectus femoris
FF SM
FF ST
FF VM
MTR RF
MTR thigh
MTR VL
FF leg central slices
FF thigh central slices
Age
Disease duration
CMTNS v2
CMTES
CMTES LL
CMTES motor LL
ONLS LL
ONLS total
MRC TA
MRC LL
1.00
0.75
0.50
0.25
0.00
−0.25
−0.50
−0.75
−1.00

B.

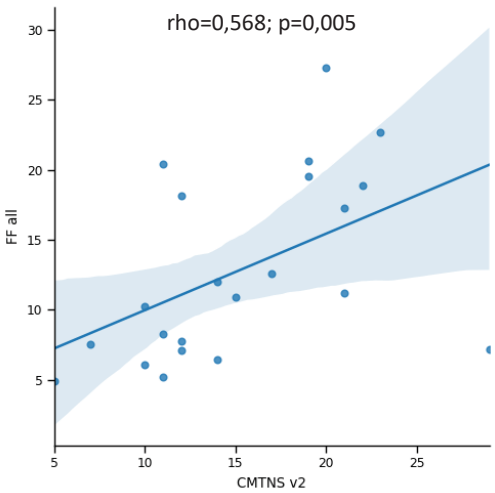
rho=0,568; p=0,005
FF all
CMTNS v2

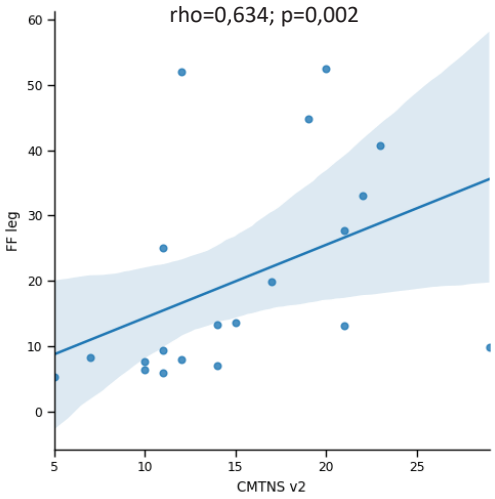
rho=0,634; p=0,002
FF leg
CMTNS v2

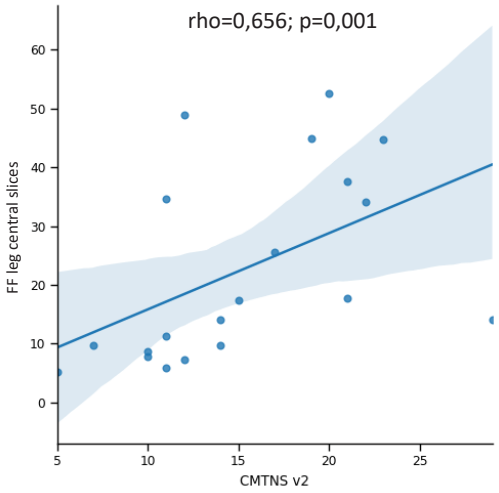
rho=0,656; p=0,001
FF leg central slices
CMTNS v2